Novel Observations on Kinetics of Nonisothermal Crystallization in Fly Ash Filled Isotactic-Polypropylene Composites

Dilip Chandra Deb Nath,[1] Sri Bandyopadhyay,[1] Aibing Yu,[2] Darryl Blackburn,[2] Chris White[2]

[1]*School of Material Science and Engineering, The University of New South Wales, Sydney, New South Wales 2052, Australia*
[2]*Research and Ash Development, Cement Australia, Brisbane, Queensland, Australia*

Received 8 December 2008; accepted 10 July 2009
DOI 10.1002/app.31186
Published online 7 October 2009 in Wiley InterScience (www.interscience.wiley.com).

ABSTRACT: A study on nonisothermal crystallization kinetics in fly ash (FA) filled isotactic-polypropylene (PP) composites has revealed some interesting phenomena. Composites made by injection moulding of PP with 0, 20, 45, and 60 wt % of FA were nonisothermally studied using differential scanning calorimetry at cooling rates 10°C, 15°C, and 20°C per min from a melt temperature of 200°C cooled to −30 °C. Whilst neat PP showed a mono modal α crystalline phase- only structure, presence of FA led to bimodal thermographs revealing partial transcrystallisation of α into β, to maximum 14%. The onset and peak crystallization temperatures of all samples decreased by ~ 3°C with each 5°C/min increase in cooling rate. Parameters such as crystal growth rate, dimensions, and activation energy were determined using a series of established models. The Avrami graphs showed that contrary to the published data, there are two sets of straight lines (a) with a lower slope at low cooling rate and (b) with a distinctly higher slope for high cooling rate. Activation energy of the materials reached a maximum at 45% FA. © 2009 Wiley Periodicals, Inc. J Appl Polym Sci 115: 1510–1517, 2010

Key words: polypropylene; fly ash; composites; crystallization and activation energy

INTRODUCTION

The semicrystalline polymer polypropylene and its composites are used in many engineering and industrial applications. The mechanical and thermal properties of PP composites depend on the degree of crystallinity and the nature of crystalline morphology, which may constitute crystallographic phases of α (monoclinic) and β (pseudohexagonal). The β phase melts at a relatively lower temperature, whereas the more stable α phase melts at a higher temperature.[1,2] In the literature, PP reinforced with inorganic natural clay shows low gas permeability, low thermal expansion coefficient, and excellent solvent and chemical resistance.[3-7] The nature of filler plays a significant role in transcrystallization of α to β form and the dimensional distribution of spherulites of PP in composites.[8] A number of studies have reported that talc,[9] kaolin,[10] carbon black,[11] calcium carbonate,[12] clay,[13] ZnO,[14] glass fibre,[15] silicon oxide,[16,17] and carbon nanotube[18] have the potential to act as enhanced nucleating agents for PP chain. Such information leads to the understanding of crystallisation kinetics in semicrystalline polymer systems which in turn control their mechanical and other engineering properties.

Various models have been proposed in the literature for the study of nonisothermal parameters in polymer matrix composites. The degree of crystallinity is generally calculated by the following equation.[19,11]

$$X_c(\%) = \Delta H_c/(1-\phi)\Delta H_m \times 100 \quad (1)$$

where ΔH_c is apparent enthalpy of crystallization, ΔH_m enthalpy of melting of 100% crystalline polymer [178 J/g for ΔH_m enthalpy of melting of 100% α-crystalline PP and 168 J/g for ΔH_m enthalpy of melting of 100% β-crystalline PP are used for calculation of crystallinity of α and β-phase PP], and Ø is the weight fraction of filler in the composite. The supercooling temperature (ΔT) can be calculated from the difference of melting and crystallization temperatures, which also characterizes the crystallization behavior of the melt.[20]

Dynamic (nonisothermal) crystallization, the common industrial route, is much more complicated than isothermal situation due to alteration of thermal environment with time. Equation (2) leads to

Correspondence to: S. Bandyopadhyay (s.bandyopadhyay@unsw.edu.au).
Contract grant sponsor: ARC (Australian Research Council); contract grant number: ARC LP0669837.

© 2009 Wiley Periodicals, Inc.

the Avrami nonisothermal crystallization kinetic parameters.[21]

$$1 - X_t = \exp(-Z_t t^n) \quad (2)$$

where X_t is the relative degree of crystallinity at time t, Z_t is crystallization constant involving both nucleation and growth rate of crystallization, n is Avrami exponent related to the crystallization dimension. The crystallization temperatures during cooling can be converted to crystallization time using eq. (3)[22]

$$t = (T_0 - T)/\Phi \quad (3)$$

where t is crystallization time, T_0 the onset crystallization temperature, T the temperature at crystallization time at t, and Φ the cooling rate from melt state. The double-logarithmic form of the above Avrami equation yields

$$\ln[-\ln(1 - X_t)] = \ln Z_t + n \ln t \quad (4)$$

According to Jeziorny model,[23] the constant $\ln Z_t$ can be expressed as

$$\ln Z_c = \ln Z_t/\Phi \quad (5)$$

where Z_c is the corrected Jeziorny crystallization constant.

Ozawa developed a new extended form of Avrami equation to determine the crystallization parameters and dimensional growth. Equation (6) was proposed for investigation of nonisothermal crystallization kinetics by integration of infinitesimally small isothermal crystallization steps.[24]

$$\ln[-\ln(1 - X_t)] = \ln K(T) - m \ln \Phi \quad (6)$$

where $K(T)$ is crystallization constant, and m is Ozawa parameter related to the crystal dimensional growth.

On the other hand, Mo[25] combined the Avrami n and Ozawa m exponents and derived another form of kinetic equation as given below:

$$\ln \Phi = \ln F(T) - a \ln t \quad (7)$$

where $F(T)$ is the crystallization constant, a the ratio of n and m exponents related to the crystallization dimension.

Kissinger model provides the following expression for the determination of activation energy in nonisothermal condition.[26,27]

$$d[\ln(\Phi/T_p^2)]/d(1/T_p) = -\Delta E/R \quad (8)$$

where T_p is the crystallization peak temperature, R is universal gas constant, and ΔE is the activation energy.

Most of the kinetics research as of date has been carried out in systems other than FA-polymer composites. Only in recent years, utilization of FA—a readily available high quantity and high quality ceramic waste—has been considered for reinforcement of polymers such as polyester,[28] epoxy,[29] and PP.[30-33] Whilst one of these papers[30] has undertaken limited thermal studies, the bulk of the publications have not investigated these important crystallization kinetics and/or the activation energy parameter of the matrix under transient cooling in the presence of FA. The objective of this paper is (a) to establish any evidence of transcrystallization in the presence of FA, and (b) to evaluate the characteristic parameters of nonisothermal crystallization kinetics in PP–FA systems using the Avrami, Jeziorny, Ozawa, and Mo models.

EXPERIMENTAL

Materials and samples preparation

a. FA sample was obtained from Gladstone Coal Fire Plant, Cement Australia, Queensland.
b. White powdery isotactic PP was procured from Martogg Company Ltd. Sydney, Australia. The ASTM D1505 −03, 10 min melt flow index (MFI) of the PP was 60, confirming that it was a low viscosity grade resin suitable for injection moulding.
c. PP–FA composite samples were fabricated by injection moulding in a Boy 15 S equipment at 210°C from premixed mixture of PP with fly ash (ball mill for 72 h) having concentrations of (a) 20, (b) 45, and (c) 60 wt % FA. Pure PP samples were also injection moulded at 210°C under similar conditions.

Thermal analysis

Melting and crystallisation studies were conducted using a Perkin Elmer Differential Scanning Calorimeter (DSC) TAC-7/DX under nitrogen atmosphere at 10, 15, and 20°C/minute heating or cooling rate in the range of −30°C to 200°C, and held for 2 min at 200°C to eliminate effects from all thermal history.[10,19] About 10–14 mg sample was sealed in a 30 μL aluminium pan, whilst another empty aluminium pan was used as the reference. The second heating and cooling peaks were taken to evaluate the melting and crystallization temperatures of PP and PP–FA composites.

RESULTS AND DISCUSSION

Crystallization behavior of neat PP and composites

The normalized nonisothermal crystallization thermographs of neat PP and model figure of composite

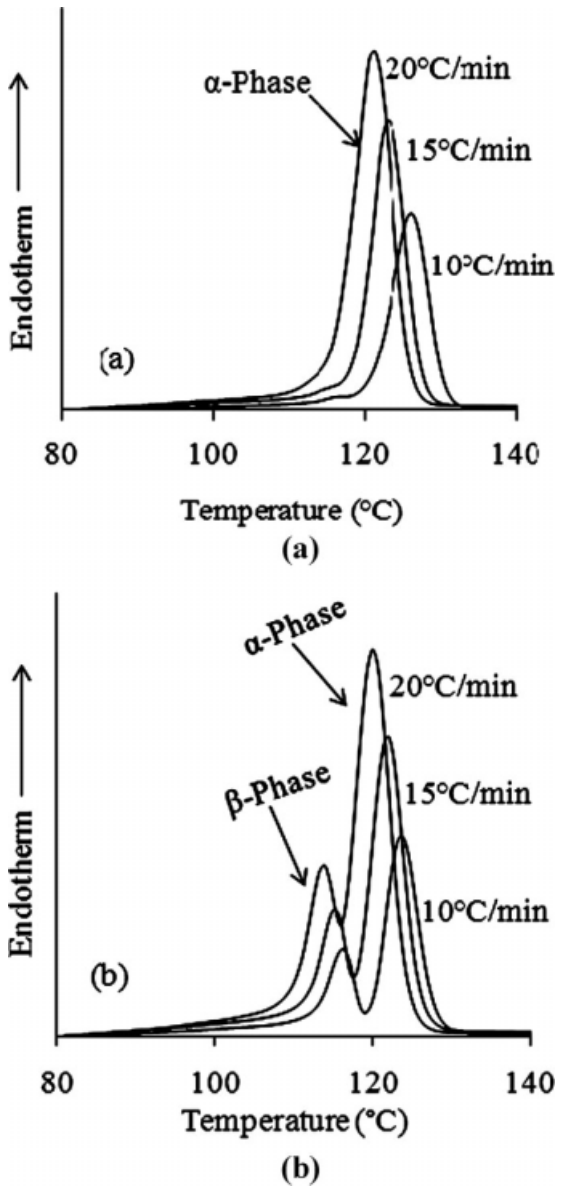

Figure 1 DSC scans of (a) neat PP and (b) 45 wt % FA composites showing non-isothermal crystallization at different cooling rates as indicated on the graphs.

45% FA at different cooling rates are presented in Figure 1(a,b). The onset, peak crystallisation, melting, and supercooling temperatures, along with calculated crystallinity using Eq. (1) were presented in Table I. From the thermograms and data presented in Figure 1 and Table I, the following general observations can be made:

a. The mono modal thermograph of neat PP in Figure 1(a) shows only α crystalline peak at 126.3°C for 10°C/min cooling rate, 123°C for 15°C/min, and 121°C at 20°C/min. In the presence of FA, these transformed into bimodal graphs [Fig. 1(b)] reflecting the partial transformation of α to β.
b. The amount of β increased with increasing FA content, and maximum 14% β was achieved with 45 wt % FA additions. β content decreased to 4% with further addition of FA to 60 wt % FA. This effect can be interpreted from diffusion and movement of molecular segments of PP suffering from hindrance at higher level of FA and increased viscosity.[20]
c. The onset and peak crystallization temperatures of the α → β peaks shift to lower positions by ∼ 2–3°C with increasing cooling rate from 10°C/min to 15°C/min and from 15°C/min to 20°C/min irrespective of FA concentration.
d. The supercooling temperatures, ΔT, increased approximately by 2–4°C in neat PP and composites on the basis of cooling rates, indicating the higher cooling rates decreases the crystallization rate. Zhang et al.[20] have reported a similar observation and attributed these to a higher rate of heterogeneous nucleation induced by FA.
e. The crystallization temperatures were converted into the crystallization time using eq. (3) and plotted in Figure 2 as the exotherms of neat PP and composites at cooling rate 10°C/min. The formation of β-crystalline PP peak apparently comes from the partial transformation of α-crystalline PP segments or from the amorphous phase of PP, therefore, the newly β-crystalline PP peak is smaller than α-crystalline peak.
f. In neat PP and composites, the onset of crystallization happens at the same time. However, in composites with higher volume fraction of FA, completion of crystallization happens sooner than for composites with lower FA content. It may thus be concluded that FA particles enhance the crystallization rate.

Avrami equation

Relative crystallinity X_t as a function of temperature was calculated by integrating Figure 1(a,b), i.e., the heat evolved during cooling of the melt (dH/dt).[22,34] The results shown in Figure 3(a,b) are the plots of $\ln[-\ln(1 - X_t)]$ as a function of $\ln t$ using eq. (4). Except for neat PP at 10 °C/min, the graphs show two straight lines with distinctly different slopes (a) the slope 1 of slow region indicating one dimension crystal lamellar growth, and (b) fast region $1 < n_2 < 3$, indicating crystals shapes approaching three dimensions. The lower slopes happened in the first half of the cooling time, whilst the higher slopes occurred in the second half of cooling. The slopes and the intercepts are displayed in Table II.

The presence of the accelerating slope is a new observation. This may have come from the disorder

TABLE I
Crystallization Behavior Polypropylene and Composites at Different Cooling Rates and the Calculated Crystallinity Using eq. (1)

FA (%)	Cooling rate (°C)	Onset temp (°C)	T_{cry} α-phase	T_m α-phase	T_{cry} β-phase	ΔT (T_m-T_{cry}) α-phase	X_α (%) α-crystal	X_β (%) β-crystal
0	10	135.2	126.3	165.0	Nil	38.7	46	Nil
	15	132.9	123.0	164.6	Nil	40.6	43	Nil
	20	131.9	121.3	163.1	Nil	42.8	42	Nil
20	10	137.3	127.3	166.4	115.6	39.1	47	1.29
	15	134.1	125.0	163.6	114.5	38.6	44	0.75
	20	133.1	122.6	163.4	113.3	40.8	42	0.65
45	10	131.7	123.6	163.4	116.3	39.7	45	14
	15	129.1	122.1	162.1	115.0	40.1	43	12
	20	128.9	120.0	162.1	113.3	42.1	40	10
60	10	134.3	123.3	168.4	117.6	43.1	46	4
	15	128.7	121.5	162.6	115.0	41.1	42	3
	20	127.3	119.3	162.7	113.3	43.5	38	1

diffusion levels of PP chains in the presence of polydisperse FA particles along with quicker cooling system - fast cooling give less time for rearrangements of molecular chains in the polymer.

Z_t values also increased steadily with increasing cooling rates. Apparently, the values of n and Z_t were influenced by the nature of nucleation and unsteady thermal condition. It is worth mentioning that work on glass fibre reinforced PP[19] and kenaf fibre-PP[35] reported the presence of a second straight line, albeit with reduced slope at increased cooling time.

Jeziorny approach

The calculated values of Z_{c1} in the primary straight line and Z_{c2} in the secondary regions using eq. (5)

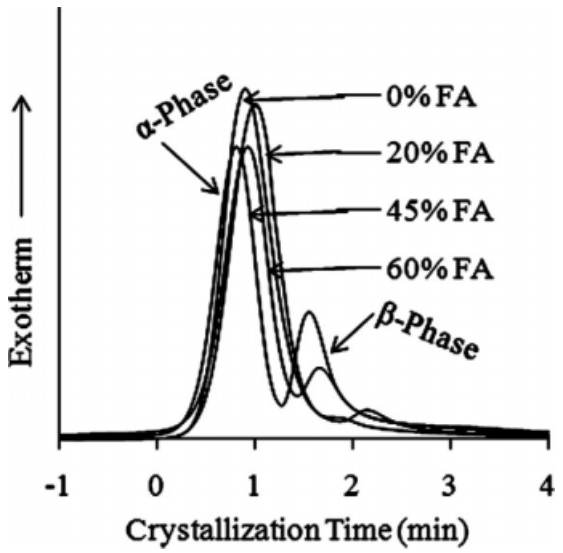

Figure 2 DSC scans of neat PP and composites against crystallization time at cooling rate 10°C/min.

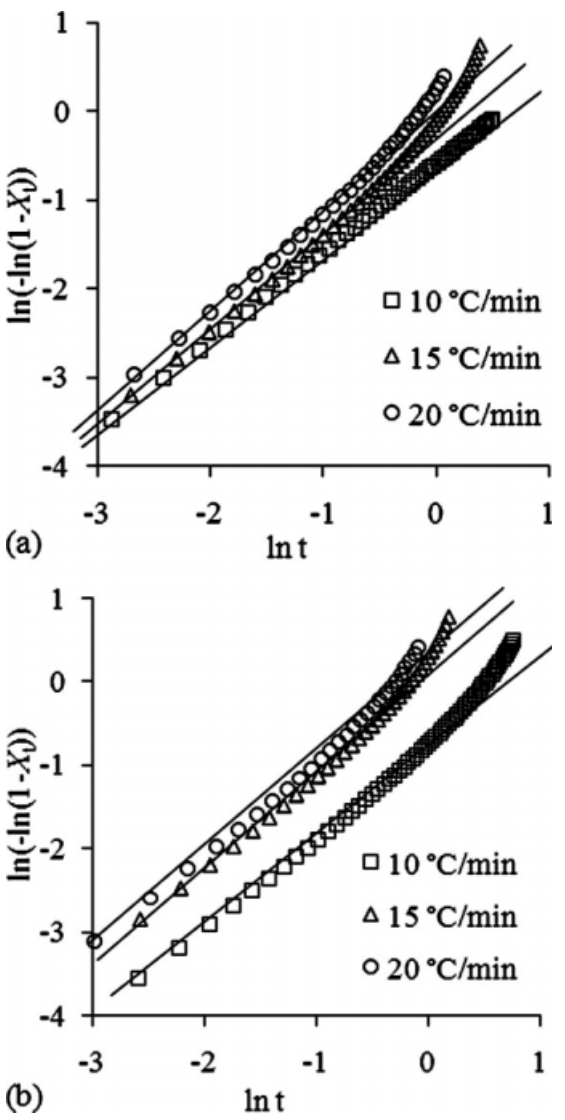

Figure 3 Avrami plots of (a) neat PP and (b) 45 wt % FA composites at different cooling rates.

TABLE II
Avrami and Jeziorny Nonisothermal Crystallization Kinetics Parameters of Neat PP and Composites [calculated by eqs. (4) and (5)]

FA (%)	Cooling rate (°C)	n_1 slope of slow regions	n_2 slope of fast regions	Z_{t1} Intercept of slow regions	Z_{t2} Intercept of fast regions	Z_{c1} slow regions	Z_{c2} fast regions
0	10	1.27	–	0.558	–	0.9433	–
	15	1.09	1.82	0.7575	0.9449	0.9816	0.9962
	20	1.05	1.61	0.8698	1.2611	0.9930	1.0116
20	10	1.07	2.48	0.6844	0.6855	0.9627	0.9629
	15	1.09	2.60	1.2375	2.5776	1.0143	1.0651
	20	1.12	2.44	1.6763	4.3692	1.0261	1.0765
45	10	1.05	1.59	0.4381	0.4531	0.9207	0.9238
	15	1.08	1.95	0.9440	1.3834	0.9961	1.0218
	20	1.05	1.53	1.0374	1.6259	1.0018	1.0246
60	10	1.03	1.86	0.5059	0.5994	0.9341	0.9501
	15	1.07	1.96	0.9852	1.6739	0.9990	1.0349
	20	1.04	2.08	1.3249	3.2504	1.0141	1.0607

are displayed in Table II. The corrected crystallization constant Z_c increased with increasing cooling rate, and is almost independent of FA content in composites, in agreement with the results obtained by other researchers.[26]

Ozawa model

The plots of $\ln[-\ln(1-X_t)]$ against $\ln\Phi$ using eq. (6) at different temperatures for the two materials are shown in Figure 4(a,b). All the plots are straight lines, confirming the applicability of the Ozawa model. The occasional changes in slope m in the plots indicate that the crystal growth dimension is altering with temperature. Values of m and $K(T)$ are displayed in Table III. A decrease in m in the range of $0 < m < 2$ and $K(T)$ with increasing temperature is observed in neat PP and 20% FA composite, whereas the increase in $K(T)$ and m in the range $0 < m < 3$ is observed in 45 and 60% FA composites. It is possible that PP and 20% FA composites enjoy two dimensional growth of crystal in a lamellar fashion, whilst in 45 and 60% FA composites the presence of large amount of FA particles causes hindrance to such planar flow, thereby resulting in localized 3-dimensional crystal growth.[11,22]

Mo equation

The plots of $\ln\Phi$ vs $\ln t$ using eq. (7) at a given degree of crystallinity in Figure 5(a,b) for neat PP and the composites show straight lines—the values of a from the slope and F(T) from the intercept are given in Table IV. It has been seen that the values of a are in the ranges of 3 to 4 in neat PP for all crystallinities, but a is below 1 in composites with slightly decreasing trend as the FA concentration increases. F(T) on the other hand increases with the degree in crystallinity in PP as well as that of the composites. There was one exception though for 80%

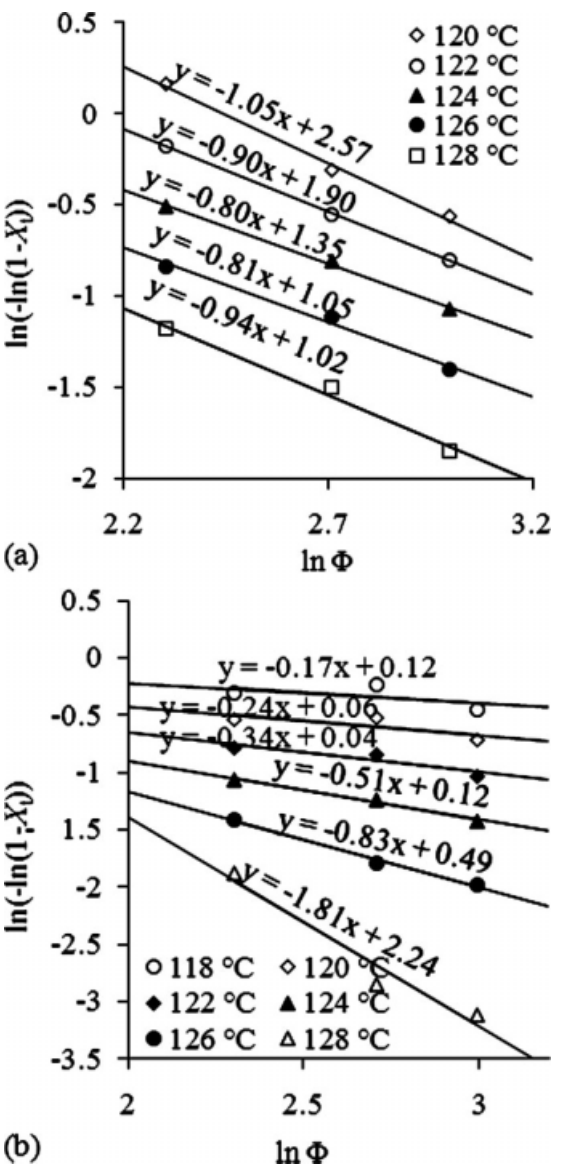

Figure 4 Ozawa plot of (a) neat PP and (b) 45 wt % FA composites at different cooling rates at selected crystallisation temperatures, 120, 122, 124, 126 and 128°C.

TABLE III
Ozawa Nonisothermal Crystallization Kinetics Parameters of Neat PP and Composites [calculated by eq. (6)]

FA (%)	Temperature (°C)	m	$K(T)$
0	118	1.48	50.65
	120	1.05	13.12
	122	0.90	6.73
	124	0.80	3.87
	126	0.81	2.86
	128	0.94	2.77
20	118	1.06	33.75
	120	1.05	33.44
	122	0.83	12.34
	124	0.81	8.39
	126	0.87	7.21
	128	1.02	7.64
	130	1.36	11.94
45	118	0.17	1.13
	120	0.24	1.06
	122	0.35	1.15
	124	0.51	1.13
	126	0.83	1.64
	128	1.81	9.39
60	116	0.85	11.89
	118	0.84	8.76
	120	1.02	10.55
	122	1.29	15.21
	124	1.16	26.31
	126	2.44	21.50

crystallinity, the F(T) values of composites are almost half of those of neat PP, indicating that the crystallization rates are faster in the presence of FA.[34]

Activation energy in composites

The original Kissinger's model[27] was established on the basis of differential thermal patterns of inorganic minerals at constant heating rates. This model was subsequently used for calculating activation energy in polymer composites during cooling and heating processes.[25,36–38]

There are several reports modifying the use of Kissinger model in cooling system. For example, the modifications of Kissinger model were done by Augis and Bennett,[39] Takhor,[40,41] Friedman,[42] and Vyazovkin and Sbirrazzuoli.[43] The calculated activation energy using former three methods did not show any big changes.[41] The present work has calculated the activation energy of neat PP and composites in heating and cooling systems using Kissinger method only.

The plots of $\ln(\Phi/T_p^2)$ as function of $1/T_p$ using eq. (8) for PP and composites are presented in Figure 6. The values of ΔE, slope, and r from the straight lines are given in Table V. The use of integral iso-conversional kinetic equation of Vyazovkin[44] in PP degradation case provided an activation energy value of 180 kJ/mol at 50% conversion, whereas our calculation using Kissinger method shows activation energy of 185 kJ/mol. The activation energy of composites are higher than that of neat PP, reaching the highest value of 251.1 kJ/mol at 45 wt % FA then showing a 10% drop to 228.6 kJ/mol when FA is 60%. The results suggest that in the presence of FA, the viscosity of the system goes up, the rearrangement of molecular segments of PP get a hindrance effect in diffusion or formation of interfacial interaction between FA and PP and it takes a higher energy to be crystallized.

The addition of filler in polymer composites changes the mechanical and thermal properties of the materials due to the formation of interfacial links between the polymer and the filler surfaces. The links, which may be physical adsorption or chemical

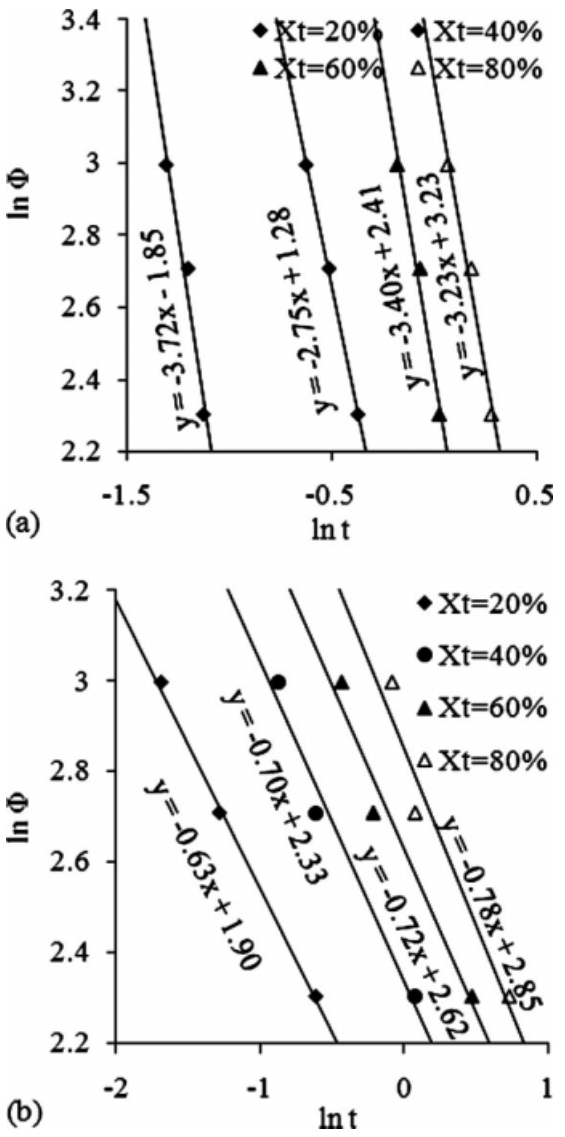

Figure 5 Mo plot of (a) neat PP and (b) 45 wt % FA composites at selected percentage crystallisation: 20%, 40 %, 60%, and 80%.

TABLE IV
Mo Nonisothermal Crystallization Kinetics Calculated by eq. (7): in Neat PP and Composite Systems

FA (%)	X_t (%)	a	$F(T)$
0	20	3.12	0.156
	40	2.75	6.410
	60	3.40	11.712
	80	3.23	25.503
20	20	0.80	4.463
	40	0.84	7.682
	60	0.84	10.730
	80	0.90	13.921
45	20	0.64	6.721
	40	0.70	10.350
	60	0.72	13.861
	80	0.78	17.372
60	20	0.67	5.983
	40	0.77	9.181
	60	0.79	12.422
	80	0.76	15.550

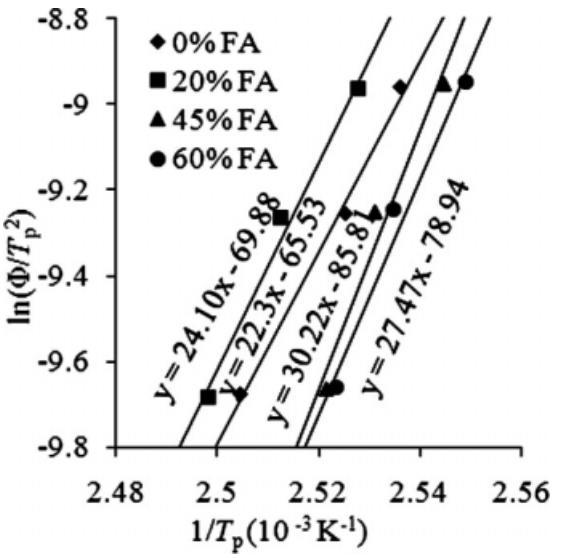

Figure 6 Kissinger plots for determination of activation energy in nonisothermal crystallization condition for neat PP and composites.

bonding, or a combination of the two, restrict the mobility of the polymer chains. Several reports have modeled the dispersion of FA or other particles in polymer composite based on the experimental results of mechanical and thermal studies, correlating these with microscopic deformation features.[45,46]

Crystallization of polymer happens from the alignment of mobile polymer chains. In the case of composites, the polymer chains may adhere onto the surface of filler, the strength of adherence solely depending on the nature and concentration of the filler. The chemical nature of the filler determines the level of interaction with the polymer chains. There are three characteristic features of polymer chains in composite materials namely, (a) immobilized, (b) intermediate and (c) mobile regions.[47]

The regions of the polymer chain are immobilized on the surface of filler due to adherence of two surfaces. The structural motions are highly constrained resulting in lack of crystallization. The intermediate region of the polymer is located a further away from the surface of the filler particles, so its dynamics are influenced by the strength of the filler-polymer interaction. The mobile region is furthest from the filler particles such that the motions are not restricted—this has the characteristics major role in crystallization.[45,47]

The authors[48] have reported higher mechanical strength of the composites at elevated temperatures, indicating presence of interfacial interaction between FA and PP. The regions of the PP chain attached onto the surface of FA reduced the mobility of PP chains during crystallization process, resulting higher activation energy as shown in this paper, Table V.

TABLE V
Activation Energy of Neat PP and Composites Calculated by eq. (8) (using R Value 0.008331447 kJ/mol)

	Activation energy in cooling time				Activation energy in heating time			
FA (%)	Cooling rate (°C)	Slope	R^2	ΔE kJ/mol	Heating rate (°C)	Slope	R^2	ΔE kJ/mol
0	10				10			
	15	22.3	0.99	185.4	15	61.4	0.83	511.5
	20				20			
20	10				10			
	15	24.1	0.98	200.4	15	38.1	0.87	317.4
	20				20			
45	10				10			
	15	30.2	0.96	251.1	15	81.1	0.83	675.6
	20				20			
60	10				10			
	15	27.5	0.98	228.6	15	19.1	0.83	159.1
	20				20			

CONCLUSION

The following conclusions are made from this study:

1. Addition of FA to PP acts as a heterogeneous β-nucleating agent and induces a secondary β-crystalline phase in the PP–FA composites—a maximum of 14% β being formed with 45 wt % FA.
2. Increasing cooling rate by 5°C/min results in 2–3°C drop in onset crystallization temperature in PP and the 3 composites.
3. All the four nonisothermal models yield good fits to the thermographs of neat PP and the composites.
4. With the Avrami plot, two slopes are observed—a slower crystallisation at low cooling rates and an almost doubled crystallisation at higher cooling rates.
5. The overall Avrami exponent n shows nonintegral number $1 < n < 3$ suggesting the existence of a size- range of three-dimensional spherulites in neat PP and PP-FA composites being formed during the cooling under the controlled rates.
6. The intercept constants Z_t, Z_c, $K(T)$, and $F(T)$ of the four models increase with increasing cooling rate in all four materials. But the values of the constants for the composites were consistently higher than those for neat PP at a given temperature.
7. The activation energy of the composites is higher than that of neat PP possibly due to enhanced viscosity of the composite systems.

References

1. Lotz, B.; Wittmann, J. C.; Lovinger, J. A. Polymer 1996, 37, 4979.
2. Li, J. X.; Cheung, W. J. Therm Anal Calorim 2000, 61, 757.
3. Messersmith, P. B.; Giannelis, E. P. J Polym Sci Part A: Polym Chem 1995, 33, 1047.
4. Usuki, A.; Kawasumi, T.; Fukushima, Y.; Okada, A. J Mater Res 1993, 8, 1179.
5. Kojima, Y.; Usuki, A.; Kawasumi, M.; Fukushima, Y.; Okada, A.; Kurauchi, T.; Kamigaito, O. J Mater Res 1993, 8, 1185.
6. Giammelis, E. P. Adv Mater 1996, 8, 29.
7. Nam, P. H.; Dubois, P.; Sun, T.; Garces, J. M.; Jerom, R. Polymer 2002, 42, 2123.
8. Acosta, J. L.; Ojeda, M. C.; Morales, E.; Linares, A. J Appl Polym Sci 1986, 32, 4119.
9. Ferrage, E.; Martin, F.; Boudet, A.; Petit, G.; Fourty, J. F.; Micoud, P.; Parseval, P. D.; Salvi, S.; Courgerette, S.; Ferret, J.; Saint-Gerard, Y.; Buratto, S.; Fortune, J. P. J Mater Sci 2002, 37, 1561.
10. Mucha, M.; Krolikowski, Z. J Therm Anal Calorim 2003, 74, 549.
11. Chen, J.; Li, X.; Wu, C. Polym J 2007, 39, 722.
12. Zhang, Q. X.; Yu, Z. Z.; Xie, X. L.; Mai, Y. W. Polymer 2004, 45, 5985.
13. Kim, B.; Lee, S. H.; Lee, D.; Ha, B.; Park, J.; Char, K. Ind Eng Chem Res 2004, 43, 6082.
14. Tang, J. G.; Wang, Y.; Liu, H. Y.; Belfiore, L. A. Polymer 2004, 4, 2081.
15. Gaceva, G. B.; Janevsky, A.; Mader, E. Polymer 2001, 42, 4409.
16. Papageorgiou, G. Z.; Achilias, D. S.; Bikiaris, D. N.; Karayannidis, G. P. Thermochim Acta 2005, 427, 117.
17. Rong, M. Z.; Zhang, M. Q.; Pan, S. L.; Lehmann, B.; Friedrich, K. Polym Int 2004, 53, 176.
18. Valentini, L.; Biagiotti, J.; Kenny, J. M.; Santucci, M. J Appl Polym Sci 2003, 87, 708.
19. Li, J. X.; Cheung, W. L.; Jia, D. Polymer 1999, 40, 1219.
20. Zhang, J.; Ding, Q.; Zhou, N. L.; Li, L.; Ma, Z. M.; Shen, J. J Appl Polym Sci 2006, 101, 2437.
21. Avrami, M. J. Chem Phys 1941, 9, 177.
22. Xu, W.; Zhai, H.; Guo, H.; Whitely, N.; Pan, W. P. J Therm Anal Calorim 2004, 78, 101.
23. Jeziorny, A. Polymer 1978, 19, 1142.
24. Ozawa, T. Polymer 1971, 12, 150.
25. Liu, T.; Mo, Z.; Wang, S.; Zhang, H. Polym Eng Sci 1997, 37, 568.
26. Xu, W.; Ge, M.; He, P. J Polym Sci Polym Phys 2002, 40, 408.
27. Kissinger, H. E. Anal Chem 1957, 29, 1702.
28. Guhanathan, S.; Sarojadevi, M. Compos Interface 2004, 11, 43.
29. Gupta, N.; Brar, B. S.; Woldesenbet, E. Bull Mater Sci 2001, 24, 219.
30. Wong, K. W. Y.; Truss, R. W. Compos Sci Technol 1994, 52, 361.
31. Wang, M.; Shen, Z.; Cai, C.; Ma, S.; Xing, Y. J Appl Polym Sci 2004, 92, 126.
32. Jarvela, P. A.; Jarvela, P. K. J Mat Sci 1996, 31, 3853.
33. Huang, X.; Hwang, J. Y.; Gillis, J. M. J Min & Mat Charact & Eng 2003, 2, 11.
34. Aella, M.; Martuscelli, E.; Sellitti, C.; Garagnani, E. J Mater Sci 1987, 22, 3185.
35. Grozdanov, A.; Burzarovska, A.; Bogoeva-Gaceva, G.; Avella, M.; Errico, M. E.; Gentile, G. Polym Eng Sci 2007, 5, 47.
36. Weng, W.; Chen, G.; Wu, D. Polymer 2003, 44, 8119.
37. Grozdanov, A.; Buzarovska, A.; Bogoeva-Gaceva, G.; Avella, M.; Errico, M. E.; Gentile, G. Polym Eng Sci 2007, 47, 745.
38. Long, Y.; Shanks, R. A.; Stachursili, Z. H. Prog Polym Sci 1995, 20, 651.
39. Augis, J. A.; Bennett, J. E. J Therm Anal 1978, 13, 283.
40. Takhor, R. L. Advances in Nucleation and Crystallization of Glasses; American Ceramics Society: Columbus, Ohio, 1971, pp 166–172.
41. Supaphol, P. J Appl Polym Sci 2000, 78, 338.
42. Friedman, R. L. J Polym Sci Part C: Polym Sympos 1964, 6, 183.
43. Vyazovkin, S.; Sbirrazzuoli, N. J Phys Chem B 2003, 107, 882.
44. Geraldo, A. J.; Filho, P.; Graciliano, E. C.; Silva, A. O. S.; Souza, M. J. B.; Araujo, A. S. Catal Today 2005, 107, 507.
45. Sridhar, V.; Xiu, Z. Z.; Xu, D.; Lee, S. H.; Kim, J. K.; Kang, D. J.; Bang, D. S. Waste Manag 2009, 29, 1058.
46. Lee, S. H.; Balasubramanian, M.; Kim, J. K. J Appl Polym Sci 2007, 106, 3209.
47. Litvinov, V. M.; Steeman, P. Macromolecules 1999, 32, 8476.
48. Nath, D. C. D.; Bandyopadhyay, S.; Yu, A.; Zeng, Q.; Das, T.; Blackburn, D.; White, C. J Mater Sci 2009, to appear.